e-PS, 2010, **7**, 147-157
ISSN: 1581-9280 web edition
ISSN: 1854-3928 print edition

www.Morana-rtd.com

e-PRESERVATIONScience
published by
MORANA RTD d.o.o.

SCIENTIFIC PAPER

LITHOL RED SALTS: CHARACTERIZATION AND DETERIORATION

Jens Stenger[1,2*], Eugene E. Kwan[3], Katherine Eremin[1], Scott Speakman[4], Dan Kirby[1], Heather Stewart[5], Shaw G. Huang[3], Alan R. Kennedy[5], Richard Newman[6], Narayan Khandekar[1]

This paper is based on a presentation at the 9th international conference of the Infrared and Raman Users' Group (IRUG) in Buenos Aires, Argentina, 3-6March 2010.

Guest editor:
Prof. Dr. Marta S. Maier.

1. Straus Center for Conservation, Harvard Art Museums, Cambridge, MA, USA
2. Center for the Technical Study of Modern Art, Harvard Art Museums, Cambridge, MA, USA
3. Department of Chemistry and Chemical Biology, Harvard University, Cambridge, MA, USA
4. Center for Materials Science and Engineering, Massachusetts Institute of Technology, USA
5. Department of Pure and Applied Chemistry, University of Strathclyde, Glasgow, UK
6. Museum of Fine Arts, Boston, MA, USA

corresponding author:
jens_stenger@harvard.edu

received: 28.05.2010
accepted: 23.11.2010

key words:
Lithol red, synthetic organic pigment, spectroscopy, crystal structure, Mark Rothko

Lithol Red salts are one of the commonest 20th century red synthetic organic pigments. We characterized the sodium, barium, and calcium Lithol Red salts with nuclear magnetic resonance spectroscopy, powder X-ray diffraction, Fourier transform infrared spectroscopy, Raman spectroscopy, and laser desorption ionization mass spectrometry. The sodium and calcium salts were synthesized and compared to commercial samples. The single crystal structure of calcium Lithol Red is reported here for the first time. Light aging experiments show that the neat powder is very lightfast but that the pigment has poor light stability within paint systems. This suggests that the binding medium facilitates the photodegradation of the pigment for the latter case.

1 Introduction

Lithol Red is a 20th century sulfonated azo pigment also known by the International Color Index name PR49. It occurs as salts of a dye formed from the coupling of 2-naphthol and Tobias acid with the counter ions sodium (PR49 or PR49:0), barium (PR49:1), calcium (PR49:2), and strontium (PR49:3), the color varying with the counter ion. The molecular structure of the pigment is illustrated in Figure 1. Lithol Red was discovered in 1899 by the Austrian chemist Paul Julius[1] at the Badische Anilin- und Soda-Fabrik (Baden Aniline and Soda Factory, BASF). It was the first β-naphthol pigment lake and was originally precipitated onto an inorganic carrier material such as barium sulfate. Later it was used in its pure form without the carrier. A review of the history, manufacture, and use of Lithol Red was published by Standeven in 2008.[2] An overview article focusing on the chemical structural types and the patent literature of metal salt azo pigments in general was published by Christie and Mackay in 2008[3] and Berrie

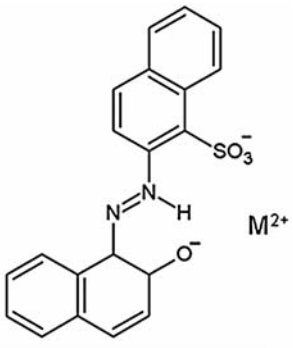

Figure 1: Molecular structure of Lithol Red salts.

and Lomax also reviewed the chemistry of azo pigments in 1997.[4] Spectrophotometric studies in the visible region of Lithol Red salts were reported in 1987 by Czajkowski.[5] He concludes that all Lithol Red salts exist in the hydrazone form and speculates that their different colors is due to differences in the crystal structure and the size of the cation.

Although commonly used in the printing industry for its brightness and bleed-resistance, Lithol Red has the reputation of being extremely light sensitive and its presence has been identified as the cause of dramatic color changes in a mural cycle by Mark Rothko, known today as his Harvard Murals.[6] Called murals only because of their size, these five paintings on canvas were on permanent display in a room with floor-to-ceiling windows in the Holyoke Center, Harvard University from 1963 to 1979. Consequently, they were exposed to high levels of natural light. The paintings display abstract forms in orange, black, blue and white on a crimson background. In 1988 Paul Whitmore determined that the pigments in the background are a mixture of ultramarine blue and Lithol Red. Recently we further analyzed the red pigment and identified it specifically as the calcium salt of Lithol Red (PR49:2). Due to the poor lightfastness of the synthetic organic Lithol Red pigment and the excessive light exposure, the background color in the paintings changed from crimson towards a light blue. The degree of the color change varies from painting to painting and also within single paintings depending on their location in the room.

When Rothko painted the Harvard Murals in 1962, Lithol Red did not have a bad reputation in technical artist's manuals. Gettens and Stout[7] wrote in 1965 that "Lithol Red has good stability to light and heat." The Bavarian paint chemist Max Doerner[8] had noted in 1934 and in later editions of his book on artist materials that several coal-tar pigments including "lithol scarlet G. are, according to Dr. Wagner, sufficiently lightproof for artists' colors." The paint industry on the other hand was ahead of the artist community with their light fastness studies. For example Vesce[9] reports in 1959 that barium and calcium Lithol Red exposed to the Florida sun for three months "are almost completely bleached". He observes this dramatic fading for several binding media such as "air dry alkyd enamel, baking super enamel, nitro cellulose lacquer and acrylic lacquer". The color change is accelerated by the addition of titanium dioxide, especially for the calcium salt.[9]

The present study focuses on the chemical characterization and photostability of Lithol Red salts. Commercial samples of the barium, and calcium salts of Lithol Red were obtained from several different manufacturers as well as one commercial sample of sodium Lithol Red, and all samples were characterized with Raman spectroscopy, Fourier transform infrared spectroscopy (FTIR), laser desorption ionization mass spectrometry (LDI-MS), pyrolysis gas chromatography mass spectrometry (PyGCMS), powder X-ray diffraction (PXRD), and nuclear magnetic resonance (NMR) spectroscopy. Several of these analytical techniques revealed that these commercial samples contained substantial amounts of impurities such as surfactants and extenders. To circumvent the impurity, the sodium and calcium salts were synthesized in-house and these synthesized forms were characterized separately. Comparison of the commercially obtained and independently synthesized pigments allowed differentiation between the signals from actual pigment and impurities in the data. Single crystal growth and X-ray diffraction was used to solve the crystal structure of calcium Lithol Red.

2 Results and Discussion

2.1 Synthesis and NMR characterization

β-Naphthol pigment lakes are industrially manufactured by first synthesizing the usually water soluble sodium salt.[1] Subsequently, the other alkaline earth salts are produced by exchange of the metal ion. The metal exchange process for the production of barium Lithol Red was studied by Czajkowski using colorimetry.[10]

For the present study, we performed the two step sequence described below. No special precautions were taken to exclude oxygen and reagents were used as received from Aldrich.

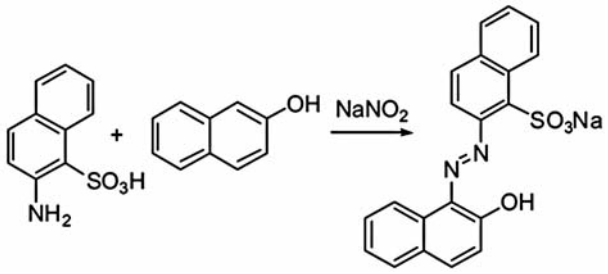

Scheme 1

2.1.1 Sodium (*E*)-2-((2-hydroxynaphthalen-1-yl)diazenyl)naphthalene-1-sulfonate (1).

Sulfonic acid (4.46 g, 20 mmol) was added to a solution of sodium hydroxide (0.84 g, 21 mmol) in 80 mL of water at room temperature. The solution was stirred vigorously until the solid dissolved.

The solution was cooled to 0 °C and sodium nitrite (1.52 g, 22 mmol) was added. After 5 min, the yellow solution was added slowly to a solution of concentrated hydrochloric acid (4.2 mL, 50 mmol, 12 M in water) in 20 mL water at 0 °C. Some chips of crushed ice were added to the hydrochloric acid solution before addition of the yellow solution to maintain the temperature of the solution below 5 °C at all times. Within moments, the solution became a neon yellow suspension. The color of this mixture darkened gradually over the course of the next 20 min. During this period, beta-naphthol (3.03 g, 21 mmol) was added to a solution of sodium hydroxide (1.20 g, 30 mmol) in 100 mL of water. After 20 min, the fine brown suspension was cooled to 0 °C. After the diazotization had proceeded for 30 min, the sodium phenolate solution was added to the diazonium salt solution. Within moments, the suspension became a vivid red color. The suspension was vigorously stirred at 0 °C for 3 h. Water was used to rinse any unreacted solids on the side of the flask into the reacting mixture. The viscous red suspension was filtered through paper using a large Büchner funnel to yield a red paste, which was then rinsed with 30 mL of chilled methanol, followed by 30 mL of water. During the rinsing, a small amount of yellow precipitate floated to the top and was removed by decantation. The washing and decanting procedure was repeated once. Finally, the resulting cake was washed with 10 mL of chilled methanol.

NMR: 500 MHz, d_6-DMSO

ID	δ^1H (ppm)	δ ^{13}C (ppm)	Hs	Multiplicity	H-H J-Couplings (Hz)
1	9.11	128.48	1	d	7.3
2	8.42	121.78	1	d	7.3
3	8.41	115.86	1	d	9.3
4	8.01	131.01	1	d	9.3
5	7.87	127.76	1	d	7.3
6	7.82	141.33	1	d	9.5
7	7.66	129.01	1	d	7.3
8	7.57	129.25	1	t	2x7.3
9	7.52	126.29	1	t	2x7.3
10	7.45	125.11	1	t	2x7.3
11	7.41	126.36	1	t	2x7.3
12	6.64	126.92	1	d	9.5

Quaternary carbons: 176.91, 148.87, 137.36, 133.96, 131.32, 130.62, 129.83, 128.00

Table 1: NMR spectroscopic data for $C_{20}H_{12}N_2O_4S$ [M+Na]$^-$.

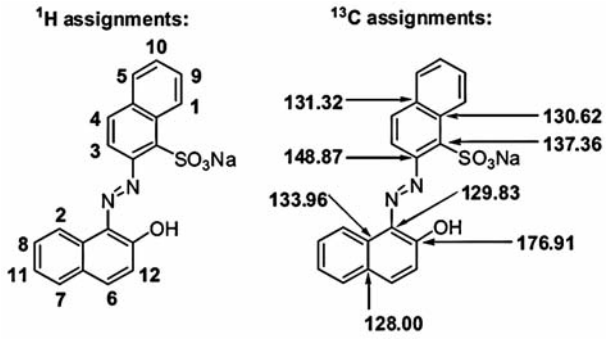

Scheme 2

Air was passed through the resulting red cake using house vacuum for 30 min to dry the solid as much as possible. The resulting red solid was collected in a round bottomed flask. The flask was rinsed with a small amount of acetone and placed under high vacuum for 72 h. The resultant dry, red solid was found to be the desired sodium salt (7.00 g, 83%) confirmed by Electrospray Ionization High Resolution Mass Spectrometry (ESI-HRMS expected for $C_{20}H_{12}N_2O_4S$ [M+Na]$^-$ 399.0406, Found: 399.0415). A summary of this compound's NMR spectroscopic data is provided in Table 1. The assignments were established by homonuclear Correlation SpectroscopY (COSY), Heteronuclear Single Quantum Coherence (HSQC) and Heteronuclear Multiple Bond Coherence (HMBC) experiments. A detailed general description of this procedure is given in reference.[11] Spectra were referenced to residual solvent peaks.

2.1.2 Calcium bis((*E*)-2-((2-hydroxynaphthalen-1-yl)diazenyl)naphthalene-1-sulfonate) (2).

The sodium salt (7.00 g, 16.6 mmol) was suspended in 250 mL of distilled water. The suspension was cooled to 0 °C. Calcium chloride (111 g, 1.00 mol) was added with vigorous stirring. During the dissolution of the salt, the temperature of the flask increased substantially. The flask was removed from the ice bath and vigorous stirring was continued for 18 h. The thick red suspension was filtered through paper using a large Büchner funnel. The cake was rinsed with 30 mL of chilled methanol. Some floating yellow impurities were removed by decantation. The cake was further rinsed with 100 mL of water followed by 50 mL of chilled methanol. Air was passed through the resulting red cake for 30 min using house vacuum to dry the solid as much as possible. The resulting red solid was collected in a round bottomed flask. The flask was rinsed with a small amount of acetone and placed under high vacuum for several days. The desired

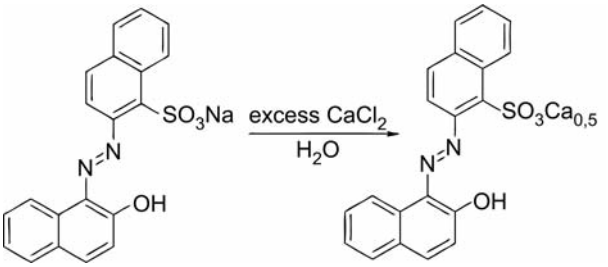

Scheme 3

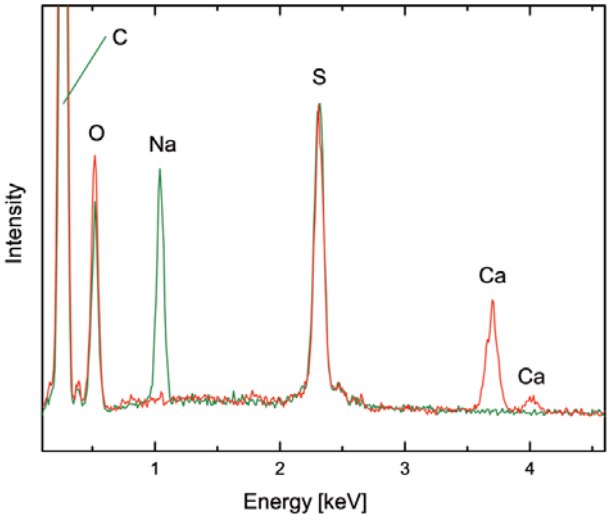

Figure 2: Energy dispersive X-ray fluorescence spectra recorded in an SEM (SEM-EDX) of the synthesized sodium (green line) and calcium (red line) Lithol Red salts.

calcium salt was isolated as a fine grained, deep red powder (6.80 g, 82%). The NMR spectroscopic properties of this compound were virtually identical to those of its sodium salt counterpart.

The yield of the metal exchange was tested in a scanning electron microscope with energy dispersive X-ray emission analysis (JEOL JSM-640LV SEM) operated at 20kV. The data illustrated in Figure 2 shows a conversion close to 100% within the measurement error.

2.2 Powder X-Ray Diffraction

2.2.1 Sample Preparation and Instrumental Parameters

Samples were prepared by dispersing a thin coating of pigment powder across the surface of a silicon zero background holder (ZBH). A thin layer of vaseline was used to help the powder adhere to the ZBH. The goal of the sample preparation method is to distribute evenly a single layer of powder particles on the ZBH. Programmable Divergence Slit was set to maintain a constant 8 mm irradiated length (the divergence slit aperture started at 0.05° and continuously increased until it was 0.95° when the scan finished). Soller Slits were used to limit axial divergence, which contributes to peak asymmetry at low angles. The overnight data were collected with 0.04 radian Soller slits; while the low angle scans were collected with 0.02 radian Soller slits. Beam width was 10 mm. The X-ray source was Cu K-alpha radiation. A diffracted-beam Ni filter was used to remove K-beta radiation.

2.2.2 Calcium Lithol Red

Figure 3 illustrates the powder X-ray diffraction patterns of calcium Lithol Red from several different commercial sources and from the synthesized compound. The samples from Lansco, EC Pigments, and Pyosa are very similar and match well with the pattern reported by Lomax.[12] It is also in good agreement with the powder pattern calculated from the single crystal structure determination (see below), except for a slight shift towards higher angles. This is to be expected since the crystal structure was determined from single crystals at low temperatures and thus with a slightly smaller unit cell. The Cappelle sample has strong signals stemming from the extenders barium sulfate and titanium dioxide. The synthesized compound also matches the commercial and calculated pattern although there are some differences in peak intensity ratios.

The peak widths of the patterns for the calcium Lithol Red from Pyosa and EC Pigments were examined more closely. In both cases, the peaks are broadened slightly compared to the silver behenate that was used as a calibration standard. For nanocrystalline materials, the peak width is

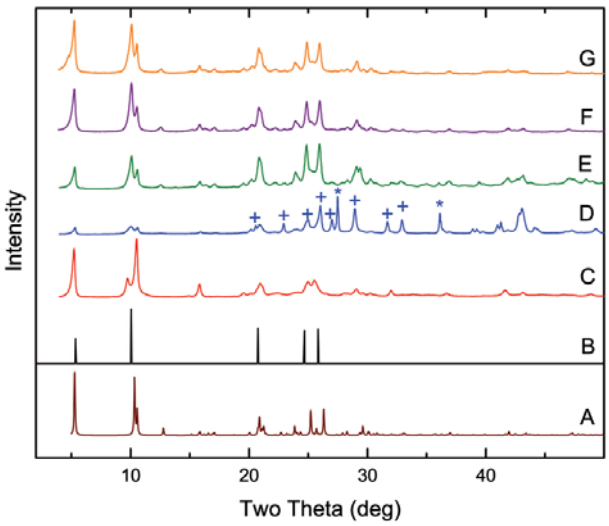

Figure 3: Powder X-ray diffraction patterns for calcium Lithol Red: A: Calculated from the single crystal structure, B: Literature reference (Suzanne Lomax,[12] C: Synthesized compound (red), D: commercial sample from Cappelle (blue), E: Lansco (green) F: EC Pigments, G: Pyosa. The Cappelle sample has strong additional signal from barium sulfate (+) and titanium dioxide (*).

inversely proportional to the crystallite size. The broadening is consistent with a material with ~48 nm crystallite size for the EC Pigment and ~56 nm for the Pyosa pigment. However, peak broadening could also be due to a high concentration of defects in the crystals of the pigment or due to lattice distortions. The data do not allow us to separate these broadening effects.

2.2.3 Other Lithol Red salts

For the sodium and barium salts the comparison between commercial and synthesized compounds is similar (not shown). Again, some of the commercial samples show additional signals from extenders. Figure 4 compares the sodium (A), calcium (B), and barium (C) Lithol Red salt powder XRD patterns. Although they all exhibit a strong peak around 5 degrees and a double peak at around 10-12 degrees, slight differences in peak positions, particularly at higher angles, mean the salts can be clearly distinguished by powder XRD.

In summary, the powder XRD patterns can be used to distinguish and identify the different Lithol Red salts and to detect adulteration with inorganic extenders such as titanium dioxide and barium sulfide. Comparison with the calculated patterns based on the crystal structure confirms the validity of the single crystal XRD approach described in the next section.

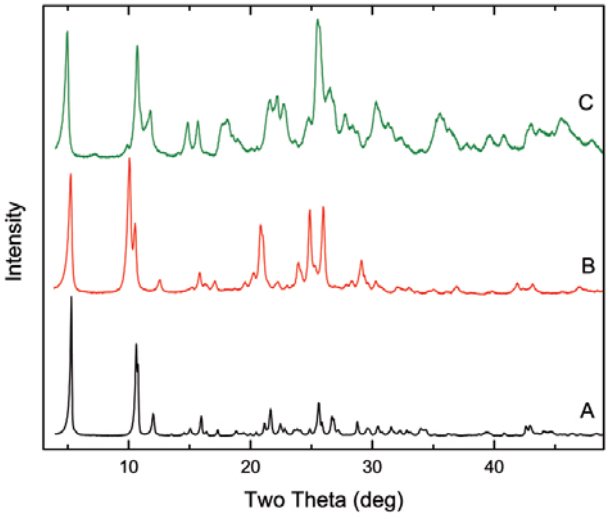

Figure 4: Powder XRD patterns for the sodium salt from Cyanamide (A, black), calcium salt from EC pigments (B, red), and barium salt from Cappelle (C, green).

2.2.4 Single Crystal Diffraction Structure of Calcium Lithol Red Dihydrate

Growing high quality single crystals of pigments and especially laked azo pigments, suitable for single crystal diffraction studies, is notoriously difficult. Problems with low solubility and anisotropic crystal habit mean that most of the few structures known for these species were derived with more specialist methods e.g. structure solution from powder diffraction, electron diffraction or the use of synchrotron radiation.[13-15] This problem was overcome for calcium Lithol Red by forming a dilute dimethylformamide solution of Sodium Lithol Red and adding a molar equivalent of $CaCl_2$ dissolved in the minimum amount of water. Left in a sealed vessel, long needle crystals formed over approximately ten days. Some of the samples obtained were too fiberous for our use, but others had a more robust habit (see Figure 5). Single crystal diffraction showed these crystals to be Calcium Lithol Red Dihydrate.[16]

The structure is disordered with both the calcium ions and the water molecules modeled with partial site occupancy factors. The displacement ellipsoids of the azo anion show features that indicate that this too is somewhat disordered, however this was not modeled. The disorder precludes detailed discussion of bond geometries, but does allow comment on connectivity. The pigment exists as the hydrazone tautomer, this is confirmed by refinement of the H atom bound to N1 (see Figure 6) and by the expected shortening and lengthening of the N-N, N-C and C-O bonds. This fits the known preference of naphthol derivatives for the hydrazone form as opposed the hydroxyl-azo form adopted by phenol derivatives.[15,17] Intramolecular hydrogen bonding between N-H and both the ketone and sulfonate groups ensures the overall planarity of the ligand (the angle between the planes defined by the C atoms of the ketone and sulfonate bearing rings is 6.1(2) °).

Each Ca atom is seven coordinate and bonds to a single terminal H_2O ligand and to four separate azo ligands. The azo ligands act as chelates using both ketone and sulfonate groups to bond to Ca. The tetrahedral sulfonate thus has O atoms in

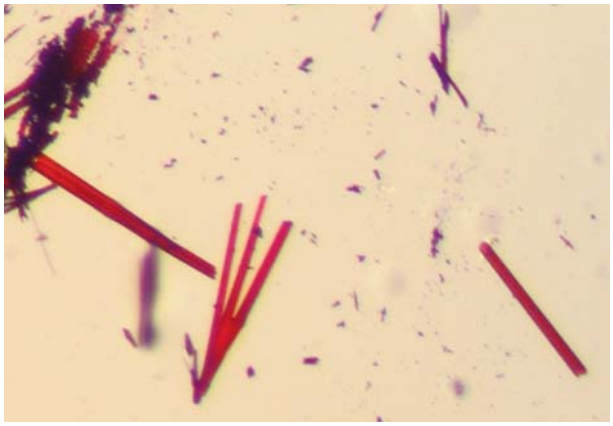

Figure 5: Crystal habit of calcium Lithol Red crystals used for single crystal diffraction. Largest crystals shown are approximately 0.4 mm long.

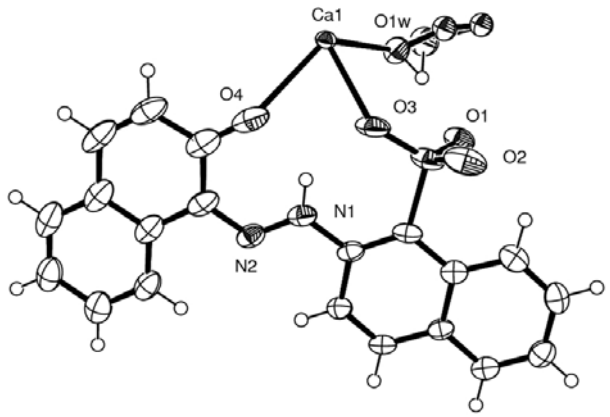

Figure 6: ORTEP view of the contents of the asymmetric unit of calcium Lithol Red with 50% probability ellipsoids. Note that the crystallographically unique portion is half of the empirical [Ca(lithol red)$_2$(OH$_2$)].H$_2$O formula. The figure shows the non-bonding water molecule as disordered over three sites.

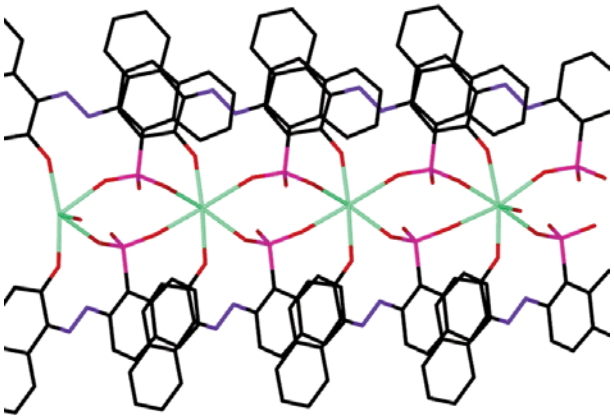

Figure 7: Part of the 1-dimensional coordination polymer formed by Ca to SO_3 bonding in the structure of Ca Lithol Red. Ca = green, S = pink, O = red, N = blue.

position to bridge to neighboring Ca atoms and hence a one-dimensional coordination polymer propagates along the crystallographic *b* direction, see Figure 7. Each link in this chain is formed from an eight-membered [CaOSOCaOSO] ring. Identical bonding motifs have been seen for Ca salts of sulfonated azo dyes.[17,18]

2.3 Fourier Transform Infrared Spectroscopy (FTIR)

FTIR spectra were recorded with a Bruker Vertex 70 spectrometer coupled to a Hyperion 3000 microscope. The samples were flattened onto a diamond cell and the infrared spectrum was measured in transmission mode between 600 cm^{-1} and 4000 cm^{-1}with a resolution of 1 cm^{-1}.

Figure 8 compares the infrared absorption spectra of the sodium, calcium and barium salts. Many vibrational bands are located in the finger print region below 1700 cm^{-1}, as expected for an organic pigment, and all three spectra are very similar in

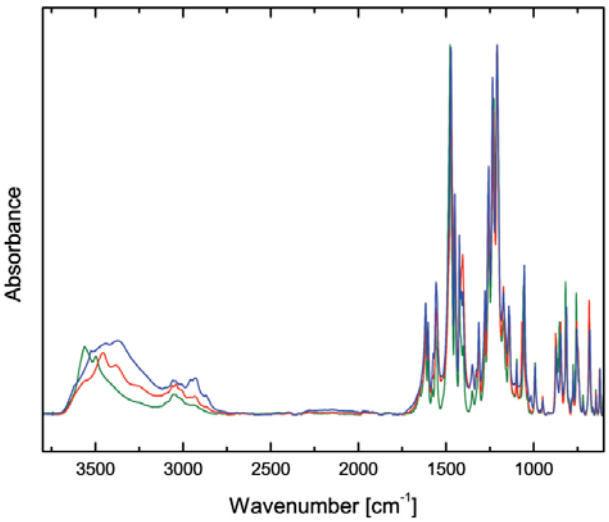

Figure 8: FTIR absorption spectra of sodium (green), barium (blue), and calcium (red) Lithol Red. The manufacturers of the three samples are Cyanamide, Pyosa, and Lansco respectively.

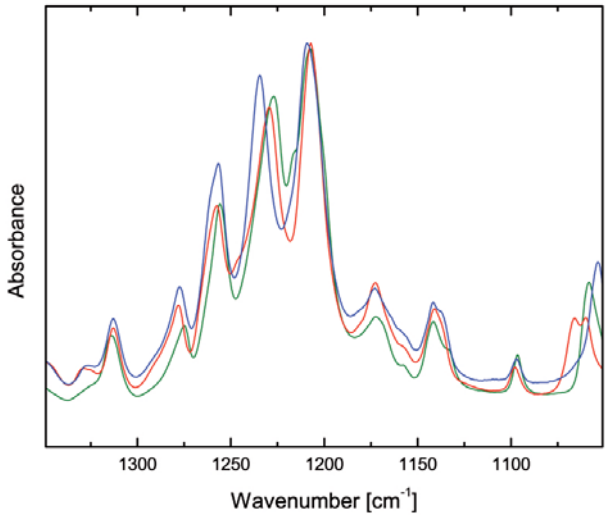

Figure 9: Detail of Figure 8. The three salts can be distinguished in the infrared spectrum by small changes in spectral peak position and intensity ratios.

that area. However, in the region around 1200 cm^{-1} the peak intensities and spectral positions are sensitive to the particular metal ion (Figure 9). These small differences are highly reproducible and independent of manufacturer and can be used to identify the particular salts by FTIR.

In the OH stretching band region around 3000-3700 cm^{-1} there are significant differences between salts, with the width of the band increasing in the order sodium, calcium and barium. The spectral position of the band maxima shifts towards lower wavenumbers in the same order. This corresponds to a shift towards stronger hydrogen bonds. The substructure in the band for all three spectra indicates that the different OH groups are hydrogen bonded in different strengths.

The aromatic C-H stretch bands above 3000 cm^{-1} are expected for this molecular compound while the

aliphatic C-H stretch bands below that frequency must stem from an additive such as surfactants based on long chain hydrocarbons.

Table 2 summarizes the peak positions for the sodium, barium, and calcium salts.

Compound	Wavenumber
FTIR spectra	
Sodium Lithol Red	606(w), 624(w), 646(w), 663(w), 684(m), 719(w), 741(sh), 750(sh), 757(m), 775(w), 819(m), 853(m), 866(s), 872(m), 949(w), 992(m), 1058(m), 1096(m), 1142(m), 1173(m), 1208(s), 1227(s), 1256(s), 1275(m), 1314(m), 1325(sh), 1350(w), 1402(m), 1416(sh), 1425(m), 1450(s), 1477(s), 1559(m), 1579(w), 1602(m), 1618(m), 1652(w)
Barium Lithol Red	601(w), 621(w), 644(w), 663(w), 680(m), 719(w), 741(sh), 755(m), 775(w), 812(m), 845(m), 873(m), 948(w), 992(m), 1016(w), 1053(m), 1097(m), 1142(m), 1173(m), 1209(s), 1235(s), 1257(s), 1278(m), 1313(m), 1326(w), 1350(w), 1404(m), 1415(m), 1424(m), 1450(s), 1472(s), 1557(m), 1573(w), 1602(m), 1616(m)
Calcium Lithol Red	602(w), 624(w), 645(w), 662(w), 684(m), 721(w), 747(s), 755(m), 775(w), 814(m), 846(m), 875(m), 949(w), 994(m), 1060(m), 1066(m), 1098(m), 1141(m), 1173(m), 1207(s), 1229(s), 1257(s), 1278(m), 1313(m), 1329(w), 1349(w), 1405(m), 1411(sh), 1424(s), 1449(s), 1471(s),1551(m), 1578(w), 1601(m), 1615(m), 1638(sh)
Raman spectra	
Sodium Lithol Red	301(m), 342(m), 357(w), 375(w), 410(m), 467(m), 480(m), 527(m), 544(w), 605(m), 644(m), 661(w), 719(s), 991(m), 1035(w), 1060(w), 1097(m), 1133(w), 1141(w), 1148(w), 1155(w), 1172(w), 1199(s), 1207(sh), 1217(s), 1235(m), 1257(m), 1324(w), 1351(s), 1403(sh), 1415(s), 1426(s), 1451(s), 1466(s), 1483(s), 1508(w), 1552(m), 1560(m), 1604(m), 1618(m)
Barium Lithol Red	301(w), 342(m), 356(w), 373(w), 410(m), 468(m), 480(m), 514(w), 528(m), 542(w), 603(m), 644(m), 660(w), 719(s), 992(m), 1035(w), 1058(w), 1098(m), 1137(m), 1147(m), 1156(w), 1173(w), 1206(s), 1216(s), 1232(s), 1258(m), 1349(s), 1413(s), 1425(s), 1451(s), 1465(s), 1484(s), 1552(m), 1558(m), 1603(m), 1618(m)
Calcium Lithol Red	300(m), 343(m), 355(sh), 373(w), 411(m), 470(m), 479(m), 514(w), 528(m), 542(w), 601(m), 644(m), 658(w), 721(s), 994(m), 1035(w), 1067(w), 1098(m), 1137(m), 1148(w), 1155(sh), 1173(w), 1208(s), 1214(s), 1226(s), 1258(m), 1279(w), 1349(s), 1409(s), 1425(s), 1451(m), 1469(s), 1483(s), 1552(m), 1559(sh), 1602(m), 1617(m)

Table 2: Peak positions in the FTIR and Raman spectra of sodium, barium and calcium Lithol Red. (w: weak, m: medium, s: strong, sh: shoulder)

2.4 Raman Spectroscopy

Raman Spectroscopy was undertaken with an excitation wavelength of 785 nm. We used a Bruker Senterra Raman microscope and a 20x objective that focused the light onto a 5 micrometer spot size with the total power of about 1 mW at the sample. A background with equal acquisition time was subtracted from each spectrum recorded for the Lithol Red salts. The resolution of all spectra was 3-5 cm^{-1}.

All six spectra acquired for the sodium, barium and calcium salts are very similar. As with the infrared spectra, it is only in the region around 1200 cm^{-1} that the spectral positions of some bands are shifted enough to distinguish between the different salts, see Figures 10 and 11. The spectra are highly reproducible and show identical bands for commercial and synthesized compounds. Pigment

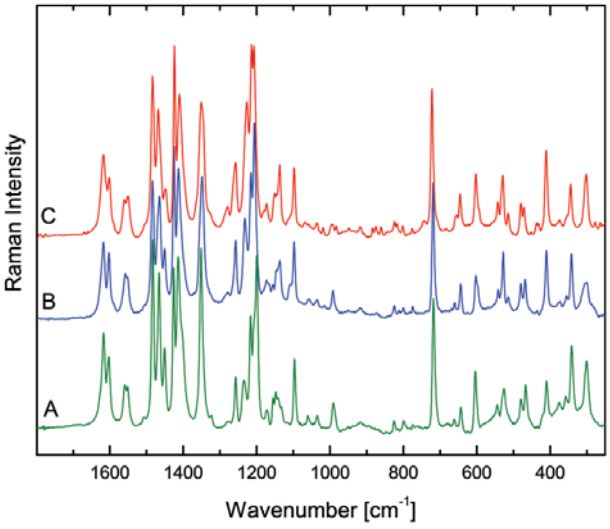

Figure 10: Raman spectra of Lithol Red salts. From bottom to top: Sodium (A, green), barium (B, blue), and calcium (C, red).

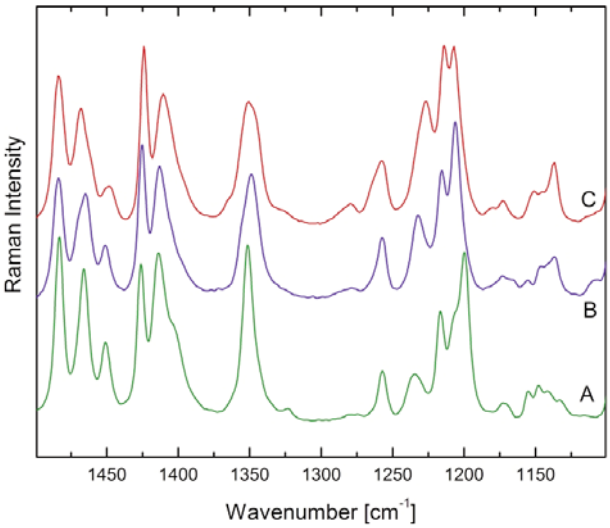

Figure 11: Detail of Figure 10. Small spectral shifts and differences in intensity ratios can be used to identify the different salts.

material found on art works including the Rothko Murals could therefore be securely identified to specific salts of Lithol Red.

A summary of the peak positions is given in Table 2. The barium Lithol Red spectral peak positions match up very well (± 1 cm^{-1}) with data reported by Vandenabeele and coworkers.[19] To our knowledge, the sodium and calcium Lithol Red Raman spectra have not been published before.

2.5 Laser Desorption Ionization Mass Spectrometry (LDI-MS)

Laser Desorption Ionization Mass Spectrometry is a recent addition to the analytical tools used in the analysis of artist materials.[20] It has quickly become a valuable approach for analysis of modern synthetic pigments. We used a Waters microMX Laser Desorption Ionization Time of Flight Mass Spectrometer (LDI-TOF-MS) operating in reflector mode to collect both positive and negative ion spectra of the Lithol Red pigments. The system used a pulsed UV laser, 337 nm wavelength, 4 ns pulse width and 5-10 Hz repetition rate. Source parameters were optimized for best resolution ($m/\Delta m$), approximately 5,000 at 646 amu, to obtain isotopic resolution of all ions. Samples were adhered to the sample plate with a 195:5 xylene:Magna (polybutyl methacrylate) mixture.

Figure 12 compares the negative ion spectra of sodium and calcium lithol red. The sodium salt shows an intense parent ion, $[M-H]^-$, 377 amu, as well as the sodium adduct, $[M+Na]^-$, 399 amu. In contrast, the calcium salt shows a very weak parent ion at 377 amu and calcium complexes at $[2M+Ca-170]^-$, 623 amu and $[2M+Ca-156]^-$, 638 amu. Fragment ions at 207 and 222 amu in both sodium and calcium salts are the result of cleavage across the diazo linkage in the dye, a common fragmentation pathway in the diazo pigments. The presence of calcium complexes but not sodium complexes may be an indication of the relative stability of these compounds.

Spectra of paint samples from art works show a similar fragmentation pattern. However, because barium sulfate or other sodium containing compounds may also be present, the specific salt is harder to identify than for the pure reference materials.

2.6 Pyrolysis Gas Chromatography Mass Spectrometry

It has been shown that PYGCMS can be an effective technique to study synthetic organic pigments,[21,22] especially for azo pigments.

In the present study, the Lithol Red salt was inserted into a quartz pyrolysis tube (CDS Analytical Inc, 465 Limestone Road, Oxford, PA 19363). The sample and tube was placed inside a platinum heating coil which was then placed into the pyrolysis injector (CDS Pyroprobe 2000) and pyrolyzed at 750°C for 10 s. The sample then passed to a DB5-MS column (30 m × 0.25 mm, 1 µm phase coating) through a split-splitless inlet (ratio 23.4:1, split flow 21 mL min^{-1}) heated to 300°C. The Agilent 6890N GC oven heated the column from an initial temperature of 40°C (1 min) to 300 °C at a ramp rate of 10 °C min^{-1} and maintained the final temperature for 20 min. The mass spectrum of the separated components was collected using an Agilent 5973 mass selective detector. Mass spec-

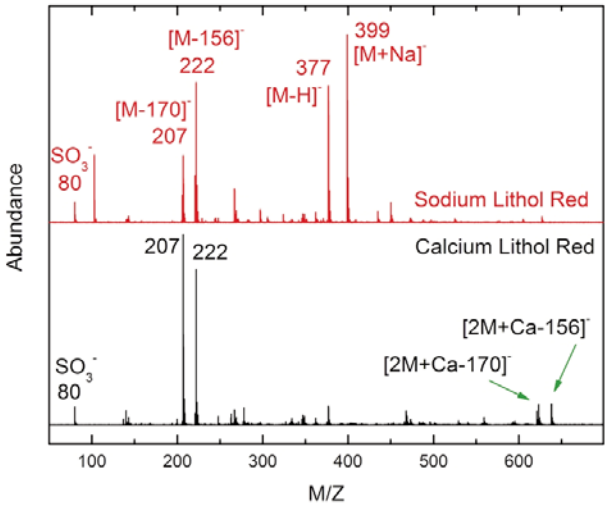

Figure 12: Laser desorption mass spectra of the two synthesized compounds sodium and calcium Lithol Red. The data was collected in negative ion mode.

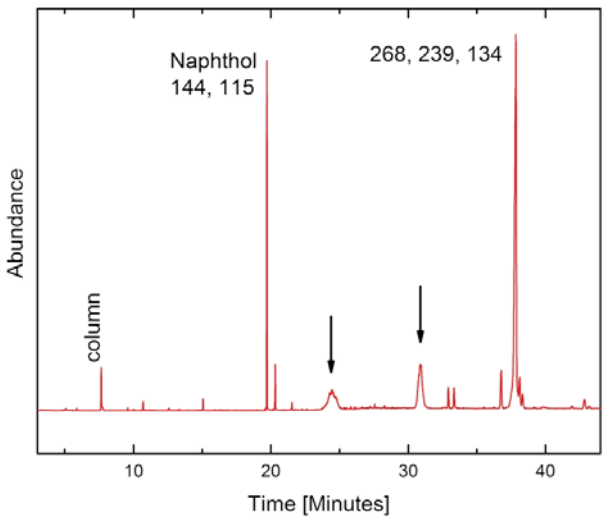

Figure 13: Pyrogram of calcium Lithol Red manufactured by Pyosa. The arrows indicate long hydrocarbon chain compounds stemming probably from a surfactant.

tra were compared to NIST and Wiley library standards.

Figure 13 shows the pyrogram of calcium Lithol Red from Pyosa. Two main peaks can be used to identify the pigment. Smaller signals labeled with arrows in the figure stem from long chain hydrocarbons, probably surfactants. They are highly water soluble and can be washed out easily with water.

Characteristic for the pigment are the signals at 19.7 min showing Naphthol and at 37.8 min yielding the main mass peaks at 268, 239, and 134.

2.7 Light aging

Light aging experiments were preformed to obtain a better understanding of the photochemistry of Lithol Red in a paint medium and to gain information on the photoproducts present on a faded art work.

A mock up of Panel One of the Harvard Murals was painted using the same materials for the background as in the original panels: Dry powder calcium Lithol Red (PYOSA) and ultramarine was added manually to warm rabbit skin glue and stirred thoroughly. This paint with watery viscosity was directly applied to the stretched canvas and resulted in a crimson background. The figure was then applied with whole egg and an orange organic pigment (as the sodium Lithol Red salt used for the original was not available in sufficient quantities). Subsequently, the painting was partially covered and exposed to light from a halogen tungsten lamp. The total exposure summed up to about 9 Mlux h and caused strong fading and blanching. A comparison of the painting before and after exposure is shown in Figure 14.

The analysis of the faded paint in the mock-up did not provide any insight into the products of the photoreaction. Inherent to the painting technique, there is very little material on the surface as the animal skin glue paint sinks into the canvas. In addition, only a small portion from the surface of the analyzed sample was actually faded and most material was unchanged.

Consequently we proceeded with a second experiment in which a thin layer of neat calcium and sodium Lithol Red powder without binder was exposed to similar light conditions in a light fading box. No visible color change was observed and no clear particles were found under the microscope. This result suggests that the photo destruction of Lithol Red in the painting is facilitated by an associated material in the paint film.

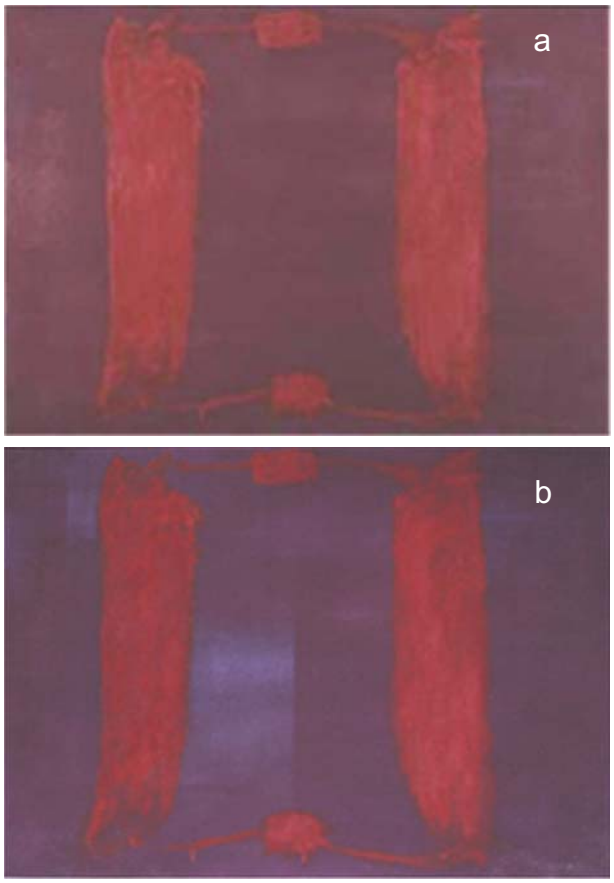

Figure 14: The mock up painting before (a) and after (b) partial light exposure in the center and the upper left corner.

Microfading experiments were performed with an instrument similar to the Whitmore design.[23] Calcium Lithol Red in rabbit skin glue (Kremer Pigmente) was painted out on white Whatman filter paper in a variety of different thickness and in mixtures with ultramarine (Kremer Pigmente). The kinetics of the reflection spectrum was recorded over time while exposing the measurement spot to light from a xenon source. Although the infrared and ultraviolet part of the xenon spectrum was removed by optical filters, the atomic emission lines remained in the illumination spectrum. In this respect the spectral power distribution is similar to the daylight simulating fluorescence lamp which was used for fading experiments on the pure powder. However, both spectra are only an approximation of the spectrum of sunlight at the Holyoke Center. The calculated color difference between the initial color and the color after exposure is plotted over time in Figure 15.

All four measurements have very similar kinetics and fall between Blue Wool 2 and 3. The addition of ultramarine blue makes no difference within the measurement error. This is interesting to note in view of recent speculation that ultramarine is the catalyst in the photodegradation of Lithol Red salts.[24] These micro fading experiment results

suggest that the binder facilitates the fading mechanism.

An additional fading experiment with the neat pigment powder was performed using a mercury lamp as a light source. Under these conditions with a substantial UV component in the illumination spectrum the sodium salt turned first from orange to red and then further darkened. FTIR spectra were taken at different stages in the experiment and are illustrated in Figure 16.

In the OH stretching band, the substructure change suggests a change in hydration or hydration geometry. The two bands at 3560 cm^{-1} and 3496 cm^{-1} disappear while a broader band appears at 3224 cm^{-1}. The appearance of asymmetric and symmetric aliphatic CH_2 stretches at 2917 cm^{-1}

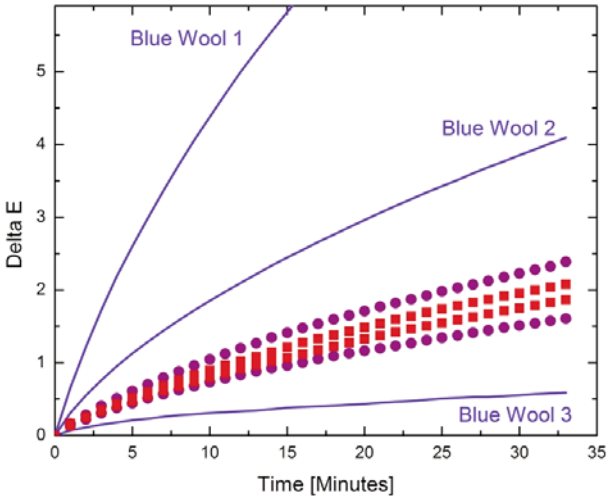

Figure 15: Color difference Delta E over time for two samples of calcium Lithol Red in rabbit skin glue (red squares) and calcium Lithol Red mixed with ultramarine in rabbit skin glue (crimson diamonds). The respective two measurements were taken on two areas of different paint thickness. The kinetics are compared to three blue wool standards.

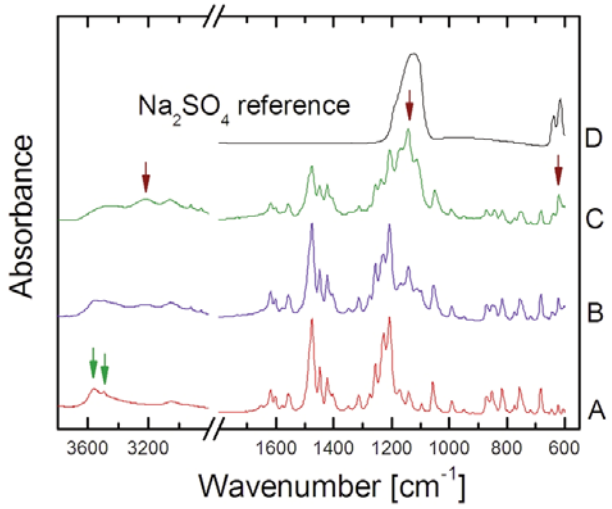

Figure 16: FTIR spectra of sodium Lithol Red A: unexposed, B: exposed, C: further exposed, D: sodium sulfate FTIR spectrum reference.

and 2850 cm^{-1} respectively may suggest a ring opening photoreaction. In the fingerprint region two additional bands appear at 1160 cm^{-1} and 620 cm^{-1}. These approximately match the bands in a reference spectrum of sodium sulfate, which may suggest that the photochemical reaction involved cleavage of the sulfonate group on the organic anion and the formation of the sodium sulfate. However, no sodium sulfate was detected by Raman spectroscopy on this altered sample.

3 Summary and Conclusions

The sodium, barium, and calcium Lithol Red salts have been characterized by nuclear magnetic resonance spectroscopy, powder X-ray diffraction, Fourier transform infrared spectroscopy, Raman spectroscopy, and laser desorption ionization mass spectrometry. Comparison of the synthesized sodium and calcium salts with commercial samples shows that the spectra and hence structures are very similar, although the latter contain large amounts of impurities causing additional features in the analytical data. Slight variations in the powder XRD, Raman and FTIR spectra of the different Lithol Red salts allow all of these techniques to be used to identify the specific salt. LDI-MS was also successful at distinguishing different salts in the pure systems but has more problems in mixed environments, such as in art works. Single crystal growth and X-ray diffraction were used to successfully determine the crystal structure of calcium Lithol Red for the first time. Light aging experiments showed that the neat powder is very lightfast but that the pigment has poor light stability within paint systems. Since the kinetics of the reaction do not appear to be affected by the presence of ultramarine, it is suggested that the presence of binding media is essential for the fading of Lithol Red. Although a possible mechanism for the photodegradation was suggested for sodium Lithol Red faded with a mercury lamp, the expected degradation products could not be found on the artworks or altered samples. Hence, further work is required to understand the mechanisms of photodegradation and the effects of binders and other pigments on the reaction.

4 Acknowledgements

Thanks to the National Crystallographic Service, University of Southampton for XRD data collection on the single crystals. We thank Paul Whitmore for providing the sample of sodium Lithol Red manufactured by Cyanamide. We are grateful for obtaining additional commercial samples from EC Pigments, Pyosa, Mexico, Lansco, NY, and

Cappelle, Belgium. JS thanks Jim Druzik for running initial microfading experiments and Sholeh Regna for providing studio space to paint the mock-up painting.

5 References

1. W. Herbst, K. Hunger, *Industrial Organic Pigments*, Wiley-VCH, Weinheim, 2004, p. 314.

2. H.A.L. Standeven, *The History and Manufacture of Lithol Red, a Pigment Used by Mark Rothko in his Seagram and Harvard Murals of the 1950s and 1960s*, Tate Papers 2008, http://www.tate.org.uk/research/tateresearch/tatepapers/08autumn/harriet-a-l-standeven.shtm (accessed 29/05/2010).

3. R.M. Christie, J.L. Mackay, *Metal salt azo pigments*, Color. Technol. 2008, **124**, 133-144.

4. B. Berrie, S.Q. Lomax, *Azo Pigments: Their History, Synthesis, Properties and Use in Artists' Materials,* in Studies in the History of Art, No. 57, National Gallery of Art, Washington DC, 1997.

5. W. Czajkowski, *Spectral Studies of Lithol Red Pigments*, Dyes Pigm. 1987, **8**, 141-150.

6. T. Hensick, P. Whitmore, in: M.B. Cohn (Ed.), *Mark Rothko's Harvard Murals*, Center for Conservation and Technical Studies, Harvard University Art Museums, Cambridge, Massachusetts, 1988, pp. 15-30.

7. R.J. Gettens, G.L. Stout, *Painting Materials: A Short Encyclopaedia*, D. Van Nostrand Company, London, 1942, reprinted 1966, p. 125.

8. M. Doerner, *The Materials of the Artist*, Harcourt, Brace and Company, New York, 1934, p. 92.

9. V.C. Vesce, *Exposure Studies of Organic Pigments in Paint Systems*, The Joseph J. Mattiello Memorial Lecture for 1959, presented at the 37th Annual Meeting of the Federation of Paint and Varnish Production Clubs in Atlantic City, New Jersey, October 23, 1959.

10. W. Czajkowski, *Studies on the reaction of the metal-exchange process during the preparation of Lithol Red R (PR49)*, Dyes Pigm. 1980, **1**, 17-25.

11. E.E. Kwan, S.G. Huang, *Structural elucidation with NMR spectroscopy: Practical strategies for organic chemists*, Eur. J. Org. Chem. 2008, **16**, 2671-2688.

12. S.Q. Lomax, *The application of x-ray powder diffraction for the analysis of synthetic organic pigments. Part 1: dry pigments*, J. Coat. Technol. Res., DOI 10.1007/s11998-009-9206-0

13. M.U. Schmidt, J. van de Streek, S.N. Ivashevskaya, *The first crystal structures of industrial laked yellow pigments determined by x-ray powder diffraction*, Chem. Eur. J. 2009, **15**, 338-341.

14. T. Gorelik, M.U. Schmidt, J. Bruning, S. Beko, U. Kolb, *Using electron diffraction to solve the crystal structure of a laked azo pigment*, Cryst. Growth Des. 2009, **9**, 3898-3903.

15. A.R. Kennedy, C. McNair, W.E. Smith, G. Chisholm and S.J. Teat, *The first azo lake pigment whose structure is characterized by single crystal diffraction*, Angew. Chem. Int. Ed. 2000, **39**, 638.

16. Crystal data for Ca Lithol Red Dihydrate: $C_{40}H_{30}CaN_4O_{10}S_2$, M_r = 830.88, monoclinic, space group C2/c: *a* = 34.655(3), *b* = 5.9449(5), *c* = 17.7137(14) Å: β = 104.661(4)˚, V = 3530.5(5) Å^3, Z = 4, λ = 0.71073 Å, μ = 0.367 mm^{-1}, T = 120(2) K; 17470 reflections, 3455 unique, R_{int} 0.0865; final refinement to convergence on F^2 gave R = 0.0771 (F, 2250 obs. data only) and R_w = 0.1860 (F^2, all data), GOF = 1.131. Full details are deposited as CCDC 776136.

17. A.R. Kennedy, M.P. Hughes, M.L. Monaghan, E. Staunton, S.J. Teat, W. E. Smith, *Supramolecular motifs in s-block bound sulfonated monoazo dyes*, J. Chem. Soc. Dalton Trans. 2001, 2199-2205.

18. A.R. Kennedy, J.B.A. Kirkhouse, K.M. McCarney, O. Puissegur, W.E. Smith, E. Staunton, S.J. Teat, J.C. Cherryman, R. James, *Supramolecular motifs in s-block metal-bound sulfonated monoazo dyes, Part 1: Structural class controlled by cation type and modulated by sulfonate aryl ring position*", Chem. Eur. J. 2004, **10**, 4606-4615.

19. P. Vandenabeele, L. Moens, H.G.M. Edwards, R. Dams, *Raman spectroscopic database of azo pigments and application to modern art studies*, J. Raman Spect. 2000, **31**, 509-517.

20. D.P. Kirby, N. Khandekar, K. Sutherland, B.A. Price, *Applications of laser desorption mass spectrometry for the study of synthetic organic pigments in works of art*, Int. J. Mass Spectrom. 2009, **284**, 115-122.

21. N. Sonoda, *Characterization of organic azo-pigments by pyrolysis gas chromatography*, Stud. Conserv., 1999, **44**, 195-208.

22. T. Learner, *Analysis of Modern Paints*, Getty Conservation Institute, 2004.

23. P.M. Whitmore, X. Pan, C. Bailie, *Predicting the fading of objects: Identification of fugitive colorants through direct nondestructive lightfastness measurements*, J. Am. Inst. Conserv. 1999, **38**, 395-409.

24. L. Carlyle, J. Boon, M. Bustin, P. Smithen, *The substance of Things*, footnote 39, page 239 in Achim Borchardt-Hume, Ed., *Rothko: The Late Series*, Tate, London, 2008.